ELSEVIER

Nuclear Instruments and Methods in Physics Research A 453 (2000) 60–70

NUCLEAR INSTRUMENTS & METHODS IN PHYSICS RESEARCH Section A

www.elsevier.nl/locate/nima

Overview: silicon vertex detectors and trackers

Peter Weilhammer

CERN EP Division, CH-1211 Geneva 23, Switzerland

Accepted 16 June 2000

Abstract

Performance requirements for Si tracking detectors for high-luminosity collider experiments are discussed. The radiation hardness of Si sensors and front-end electronics for the readout of Si detectors is reviewed. Some typical experimental results on radiation hardness are presented. The basic ingredients needed for the construction of Si trackers are described. Some performance results are shown. A very short discussion of mechanical support structures and alignment methods is given. © 2000 Published by Elsevier Science B.V. All rights reserved.

Keywords: Si sensors; Tracking; Radiation hardness; Front-end electronics; High luminosity hadron colliders

1. Introduction

The advent of heavy particles composed of massive b- and c-quarks in the 1970s has driven an intensive development program in high-energy physics of position sensitive Si radiation sensors with the best-possible spatial resolution. With decay times around 10^{-12} s of these particles the transverse decay lengths $c\tau$ of about 150–500 μm have to be measured with good spatial resolution. This provides an efficient tool to separate these heavy particles with low-production cross-sections from other events, using the finite decay vertex distance. For good discrimination a point precision of better than 10 μm is required.

The first implementations of Si vertex detectors in fixed target experiments covered areas of typically a few tenths of a square metre. The second generation of vertex detectors was developed for all experiments at e^+e^- colliders (LEP at CERN, SLC at SLAC, CESR at Cornell), for the CDF experiment at Fermilab, for Zeus and the H1 experiment at DESY and most recently for the B-factories at SLAC and at KEK. These detectors have typically a size of 0.5–1.5 m^2 and use very advanced Si trip sensors and VLSI front-end electronics. Almost all physics results, from the discovery of the t quark to the confirmation of the predictions of the Standard Model to highest precision, rely heavily on the performance of these vertex detectors.

In the past the vertexing aspect of Si detectors was predominant. In the new generation of high-luminosity collider experiments with extensive solid angle coverage, tracking inside the calorimeters will be done with Si trackers covering large areas with millions of channels. The main purpose of these Si tracking systems is a precise determination of the momentum of high-p_T, high-energy particles, which are believed to be signatures of new physics phenomena. Vertex detection in these tracking systems will be performed by the inner most layers of pixel detectors.

In this overview, performance requirements for Si vertex detectors and trackers, radiation hardness

E-mail address: weilhammer@cern.ch (P. Weilhammer).

PII: S0168-9002(00)00607-0

of sensors and front-end electronics, and required properties of sensors, front-end electronics, mechanics, cooling and alignment will be discussed. Some typical examples will be shown.

2. Performance requirements

The requirements are somewhat different for Si sensors depending on the application. The spatial resolution is clearly the most important parameter for vertex detection. The best resolution achieved with Si strip detectors is $\sigma = 1.4\,\mu m$ using a 300 μm thick sensor with 25 μm pitch and 50 μm readout pitch equipped with low noise [1], slow (μs peaking time) readout electronics (Fig. 1).

The important quantity for efficient and precise b-tagging and b-trigger capability is the resolution on the impact parameter d, the transverse distance of primary vertex and decay vertex. Examples from presently running experiments are: DELPHI using double-sided strip detectors which achieved $\sigma_d(r\varphi) = 21\,\mu m$ and $\sigma_d(z) = 36\,\mu m$ for 90° $Z^\circ \to \mu^+\mu^-$ decays [4]. The SLD vertex detector SVD3 using Charged Coupled Devices, has measured an asymptotic impact parameter resolution of $\sigma_d(r\phi) = 9\,\mu m$ and $\sigma_d(z) = 14\,\mu m$. The goal with the ATLAS pixel detector is $\sigma_d(r\varphi) = 11\,\mu m$ asymptotically. For vertex detectors at asymmetric B factories longitudinal vertex separation for 2 B meson vertices of $\sigma_d(z)$ better than 130 μm is required. In all cases, the impact parameter resolution depends not only on the intrinsic Si sensor resolution but equally on precise alignment of the whole detector and minimisation of multiple scattering.

For stand-along tracking applications in the detectors at future high-luminosity colliders, LHC and upgraded TEVATRON, good efficiency in track reconstruction, low-noise occupancy and good pattern recognition capability are likely to play the biggest role. A spatial point resolution of $\sigma = 15$–$25\,\mu m$ is sufficient to obtain the required resolution in transverse momentum up to the TeV range, e.g. in CMS a transverse momentum resolution of $\delta p_t/p_t \sim 15 p_t$ (TeV)% is specified.

The most challenging task for vertex detectors of the future is triggering. The LHCb and BTEV experiments plan to use track information in the level

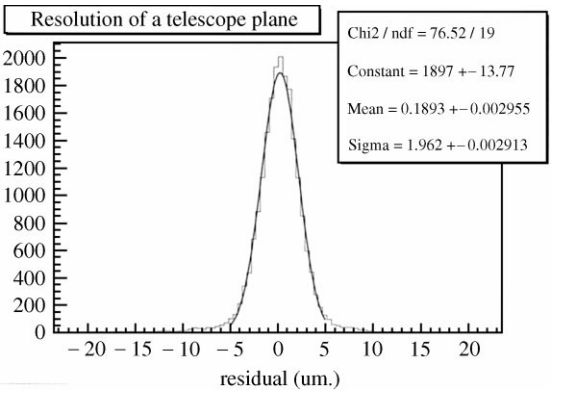

Fig. 1. Spatial resolution obtained with Si strip detectors [2,3]. The distribution shows residuals of a projected track and the measured coordinate in the DUT. $\sigma_{point} = \sigma_{res}/\sqrt{2} = 1.4\,\mu m$.

1 trigger. Online track reconstruction at event rates of 1 MHz using fast algorithms and processor arrays is envisaged. The goals are to trigger on tracks with large transverse momentum and on reconstructed secondary vertices.

3. Radiation hardness of sensors and front-end electronics

While the first generation Si vertex detectors in fixed target experiments, and in e^+e^- collider experiments did not have too many problems from radiation damage (with the exception of some small accidents with lost beams hitting a few detectors), the high particle fluences generated by the very high-luminosity pp interactions at LHC, TEVATRON and HERA-B are a tremendous problem. There is some concern about radiation damage in Si vertex detectors in B-factory experiments, but the problem is an order of magnitude smaller than predicted for high-luminosity hadron colliders. A first indication of radiation damage to front-end electronics were seen in the inner layer of the first CDF vertex detector [5]. Simulations for fluences around the LHC interaction regions predict values shown in Table 1.

More than 10 years of R&D on the effects of radiation on the response of Si sensors have demonstrated that Si sensors have very good radiation resistance. Similar studies have led to a good

Table 1
Expected fluences of diffferent particles for 10 years of full luminosity running at $L = 10^{34}\,\mathrm{cm}^{-2}\,\mathrm{s}^{-1}$

Radius	π	p	n	Total
	[$\times 10^{14}$ particle/cm^2]			
10 cm	5	1	1.1	~ 8
30 cm	1	0.1	0.8	~ 2

understanding of radiation hardness of front-end electronics and to new developments of radiation hard technologies.

3.1. Sensors

Limits of survival for Si sensors are determined by the amount of non-ionising energy loss deposited in the high resistive Si bulk by the traversing particles [6]. The major effects responsible for final failure of a Si sensor are

(i) Space charge inversion in the n-type material (from positive to negative space charge) with increasing number of lattice defects, which leads to effective p-type doping of a sensor under bias. This effective p-type doping increases with fluence and with time even after irradiation (anti-annealing).
(ii) Increase of leakage current with increasing fluence.
(iii) Decrease of free carrier lifetime by charge trapping which leads to signal loss.

An example of space-charge inversion resulting in an increase of the effective doping concentration of more than two orders of magnitude up to a fluence of 10^{15} p/cm^2 is shown in Fig. 2.

Intensive research into these effects has led to Si sensor technologies which finally improve the radiation hardness of Si sensors. It has been shown that Si bulk material with high oxygen concentration exhibits a smaller increase of depletion voltage equivalent to a reduced increase in p-doping concentration by about a factor two compared with normal material [Fig. 3]. This difference pertains even after full anti-annealing.

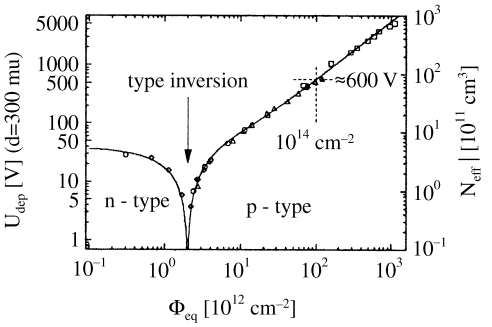

Fig. 2. Change in the depletion voltage with the absolute effective doping concentration measured after irradiation ϕ_{eq} is fluence normalized to 1 MeV neutrons [7].

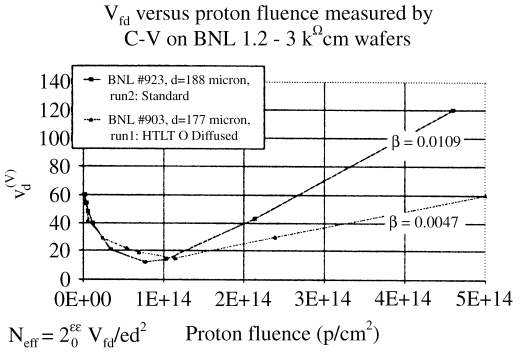

Fig. 3. Full depletion voltage measured on irradiated Si diodes with enriched oxygen concentration.

The effect of lattice damage on leakage current is shown in Fig. 4. Many diodes have been irradiated to different equivalent fluences. The volume current increases linearly with equivalent fluence.

An example for signal loss in a Si strip sensor due to trapping in the radiation-damaged material is shown in Fig. 5.

Both detectors were read out with the fast SCTA pipeline chip [9,10] with 25 ns peaking time. The full deposited charge is sampled at about 60 V above depletion voltage for the non-irradiated detector p20. After irradiation one has to apply on the detector p7, an over-voltage above depletion of about 250 V in order to get the full charge from the detector.

The importance of precise tracking very close to the LHC beam pipe has triggered research into

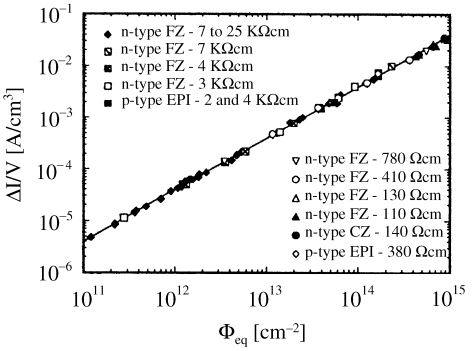

Fig. 4. Fluence dependence of leakage current for Si diodes produced from different starting materials [8].

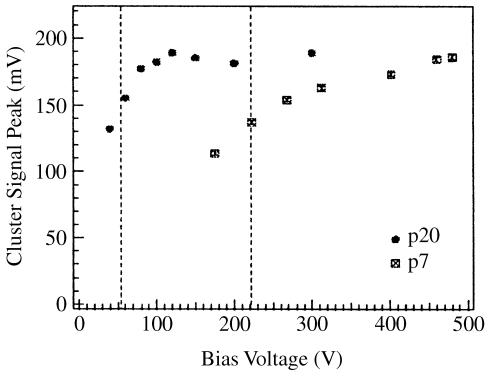

Fig. 5. Cluster signals from two strip detectors with 60 mm long strips readout with a fast LHC analogue front-end, the SCTA chip. In the non-irradiated detector (p20) 50 V over depletion are sufficient to measure the total charge without ballistic deficit. The detector irradiated with 3×10^{14} p/cm^2 (p7) needs 250 V over-depletion.

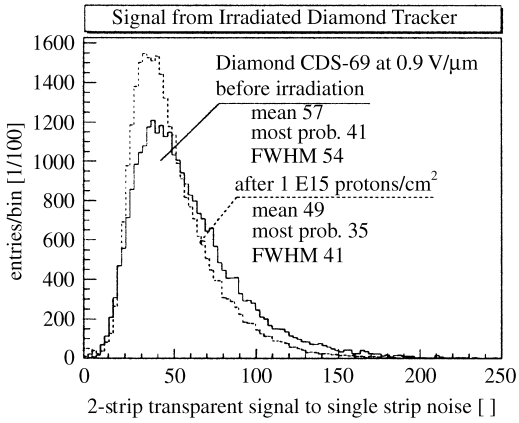

Fig. 6. Landau distribution measured with a CVD diamond strip detector before and after proton irradiation up to a fluence of 10^{15} p/cm^2.

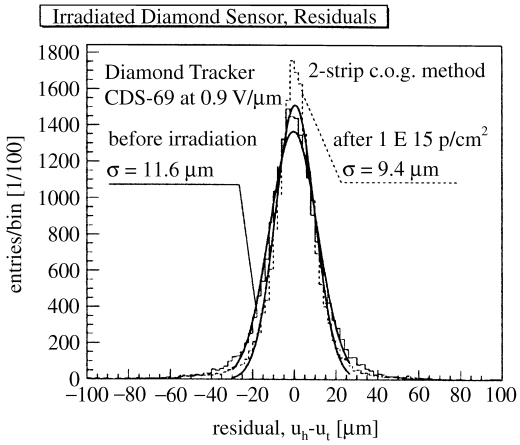

Fig. 7. Spatial resolution of CVD diamond strip detectors before and after irradiation.

other possible sensor materials like CVD diamond and SiC. Fig. 6 shows Landau distributions measured with a diamond strip detector with 50 μm pitch before and after irradiation at a fluence of 10^{15} p/cm^2 and Fig. 7, the spatial resolution measured with the same detector. The CVD substrate is produced by DeBeers Industrial Diamond Division.[1] Both the amount of charge collected and the spatial resolution change very little. This demonstrates that one could hope to have radiation sensors made from CVD diamond which can survive up to a fluence of several 10^{15} p/cm^2.

3.2. Front-end electronics

As for Si sensors a series of research efforts have gone into developing or testing radiation-hard VLSI electronics to be used for the readout of Si sensors. This is of particular importance for pixel detectors at small radii where the front-end electronics will receive very high radiation doses in

[1] DeBeers Industrial Diamond Division Ltd., Charters, Sunninghill, Ascot, Berkshire SL5 9PX, England.

excess of 10^{15} charged particles/cm^2. Most available technologies have been evaluated [11,12]. For applications in LHC and TEVATRON, the Honeywell 0.8 μm bulk SOI CMOS (SIMOX)[2] and the TEMIC DMILL BICMOS (SIMOX)[3] processes have been shown to allow the production of front-end circuits which can survive up to fluences of several 10^{14} p/cm^2 with the required performance. Limits for bipolar devices are β degradation to values below 20 at around 5×10^{14} p/cm^2. Limits for CMOS are doses of 10–20 Mrad.

The most promising technology for highest radiation hardness maybe, however, the recent commercially available deep sub-micron processes. First studies show that circuits built in 0.25 and 0.35 μm technology are not affected in their performance after irradiation up to 30 Mrad [13]. The main reason for this "in-built" radiation hardness is the very thin gate oxide. Values of measured flat band voltage shifts after irradiation increase proportional to the square of the gate oxide thickness above a thickness of about 60 nm.

Below 20 nm the flat band voltage shift decreases very rapidly with decreasing oxide thickness [14] (Fig. 8). For 6 nm oxide thickness V_{FB} is more than 2 orders of magnitude below the t_{OX}^2 line. This effect can be explained by the quantum mechanical tunnelling of trapped oxide charge and consequent charge neutralisation in the underlying Si. It has been shown that special layout techniques can in addition eliminate radiation-induced leakage [13]. An example of such techniques, a gate enclosed NMOS device with guard ring structure, is shown in Fig. 9. Source-drain leakage currents do not change up to 30 Mrad.

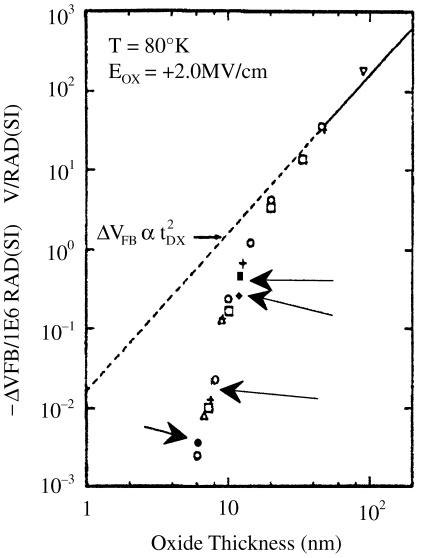

Fig. 8. Flat band voltage shifts measured as a function of gate oxide thickness after irradiation dose of 1 Mrad [14].

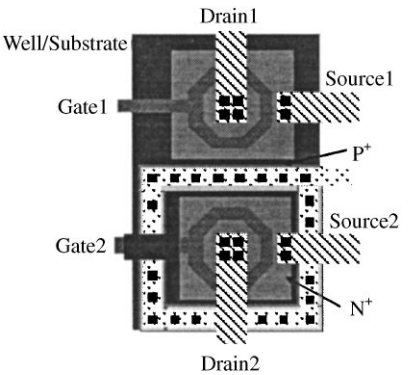

Fig. 9. Gate-enclosed NMOS device. The enclosed structure suppresses parasitic source-drain leakage current [13].

4. Basic ingredients of vertex detectors and trackers

In the following, an overview will be given of important features of sensors, front-end electronics and very shortly of mechanical support structures. The most important properties of these ingredients will be discussed and some typical examples will be mentioned.

4.1. Si sensors

So far all vertex detectors have used Si sensors made from high resistive material. Other materials have been investigated or are under study, mainly with the goal to find materials with radiation

[2] Honeywell Solid State Electronics Center, Honeywell Technology Center, Plymouth, MN 55441, USA.

[3] TEMIC Semiconductors, TEMIC France SNC, 3 av. du Cendre, B.P. 309, 78054, St. Quentin en Yvelines, France.

hardness better than Si. GaAs has very good radiation hardness for neutrons but is damaged more than Si after pion irradiations [15]. Oxygenated Si has been shown to have better radiation resistance than normal Si w.r.t. the full depletion voltage after irradiation and also after the anti-annealing treatment [16].

CVD diamond is under study and there are indications that it can be used beyond fluencies of 10^{15} particles/cm^2 [17].

The types of sensors which are most commonly used in vertex detectors are: single-sided and double-sided microstrip detectors, pixel detectors, pad detectors, Si drift chambers and Charge Coupled Devices (CCD).

4.1.1. Si strip sensors

The technology which was mostly used in LEP and TEVATRON experiments are sensors with strip patterns on both sides. The very big vertex detectors and trackers for future collider and space experiments, covering typically up to 100 m^2 area, propose single-sided p^+n sensors. On double-sided detectors the p-side has p^+ (Boron) implants in the form of strips, which provide the p^+n junction. The n-side has orthogonal strips implanted with phosphorus providing ohmic contact. Ohmic shorts between strips on the n-side are prevented by p-stop implants or by p-spray implants. A typical structure on the n-side is shown in Fig. 10.

Bias resistors are integrated on the sensor. These are either poly-silicon lines with a doping density tuned to produce a resistance between 100 kΩ and several 100 MΩ. A widely used technology are punch-through resistors which gave a very high dynamic resistance with $R_{dyn} \sim 1/I_{leak}$. For good strip detectors leakage currents can be as low as 100 pA for a 6 cm long strip which gives $R_{dyn} \sim 1\,G\Omega$. The coupling of the p^+n junction strips and the n^+n contact strips to the front-end electronics can be DC or AC. Integrated AC-coupling uses SiO_2 or SiO_2/Si_3N_4 isolation layers between implants and metal strip. AC coupling can also be achieved by means of a separate bias chip on a glass substrate, which carries both the capacitors and the poly-silicon resistors. Guard ring structures around the periphery of the sensor play an important role to allow operation at very high

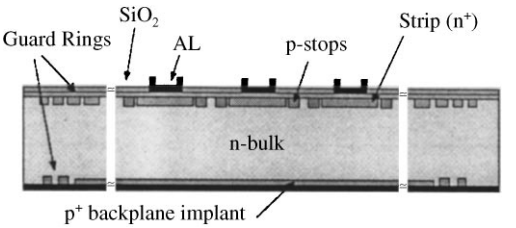

Fig. 10. Layout of a strip detector with strips on n^+-side with p-stop ohmic separation.

voltages. Optimisation of multi-guard ring structures have become important for operation of these sensors in the environment of high luminosity collider experiments. This is due to the fact that after heavy irradiation and reverse annealing Si sensors need several 100 V for full depletion. In addition, a substantial over-depletion voltage is necessary to avoid ballistic charge deficit at very short shaping times.

4.1.2. Si pixel sensors

The technology used for pixel sensors is in many ways identical to strip sensor technology. Pixel detectors are planned for installation very close to the interaction region in an extremely severe radiation environment. Most presently developed systems need sensor material and a layout that yields very high radiation hardness. For this reason, a widely pursued option is Si n^+n pixels with p-spray isolation between adjacent pixels fabricated on oxygenated Si substrate. The reason for this choice is space-charge inversion for fluences above 10^{14} charged particles/cm^2. For inverted sensors the space charge region develops from the n-side into the bulk when voltage is applied. For readout on the n^+ side charge carriers move close to the readout electrodes also when the detector is not fully depleted.

The geometry of pixel sensors is determined by minimum pixel size of the readout chip that allows to accommodate all the necessary functions, which is of the order of 20,000 μm^2. Choices are between square pixels of 150 μm × 150 μm and rectangular shaped pixels of 50 μm × 400 μm. A square pixel geometry can achieve better resolution than digital if one makes use of the Hall angle in the charge

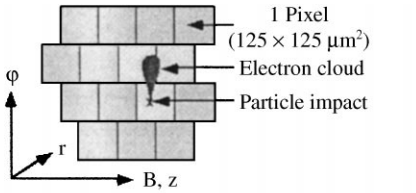

Fig. 3.2: Barrel pixel arrays and charge spread due to the magnetic field.

Fig. 11. Charge distribution in pixels in CMS experiment.

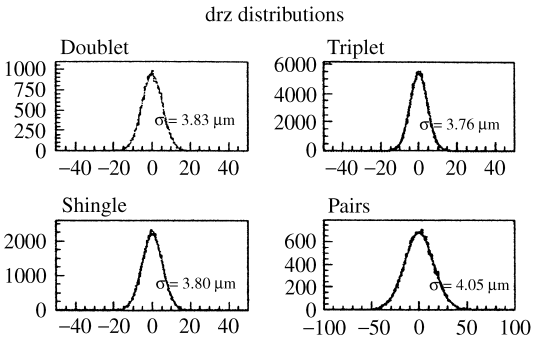

Fig. 12. Spatial resolution obtained with the SLD SVD3 vertex detector.

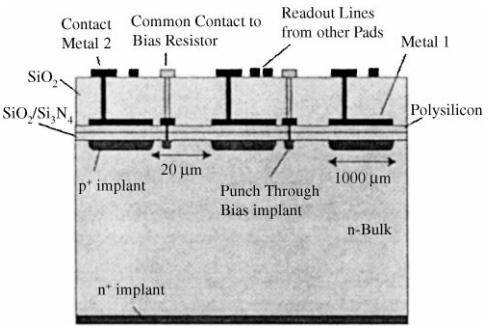

Fig. 13. A schematic view of a Si pad detector.

transport in strong magnetic fields. This scheme is implemented in the CMS pixel detector. Fig. 11 shows the influence of the strong magnetic field of 4 T on the distribution of the charge of the electron cloud over the pixels.

4.1.3. Charge Coupled Devices

Charge Coupled Devices (CCD) have been used for a long time for charge storage and transfer and most importantly as optical sensors, mostly in video cameras. The principle of a CCD is to transfer charge generated in a thin depleted region of the CCD to the edge of the device using gate electrodes on top of the oxide. Charge arriving in the edge row (linear CCD) is shifted cell by cell onto a single output electrode.

About 20 years ago, specially selected commercial devices were developed as particle detectors in high-energy physics [18]. A very large device has been built for vertex detection in the SLD experiment at the SLAC linear collider [19]. Large area MOS CCDs with 80 mm × 16 mm and a pixel size of 20 μm × 20 μm have been used. Of all two-dimensional Si devices it has the best spatial resolution (Fig. 12).

4.1.4. Si pad detectors

In applications where pixel dimensions of about 1 mm × 1 mm are required, it is more economic to route the readout of each pad to the periphery of the sensor using double metal technology [20] as shown schematically in Fig. 13. One application is a ring multiplicity detector in the PHOBOS experiment at RHIC. It will be used to measure multiplicities and to perform 3D tracking in high-energy ion–ion collisions.

4.1.5. Si drift detector

A Si drift detector [21] employs p^+n junction implants in the form of strips on both surfaces of the sensor. The device is depleted from both sides by applying a negative voltage on the p^+ strips. This voltage is regularly graded along the detector by voltage dividers between the strips which creates an electric field component parallel to the surface of the sensor. The electrons will be collected in a potential minimum in the middle of the sensor and move in the drift field towards readout anodes formed by n^+ implants (Fig. 14).

The measurement of the arrival time and the implementation of segmented collection anodes provides two-dimensional position information. The collection anodes have in general very low capacitance. Important issues for good performance are material uniformity, defect-less material over the whole wafer, precise temperature control,

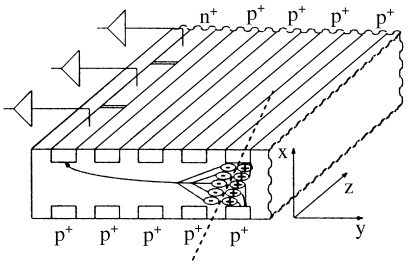

Fig. 14. Schematic view of a Si drift detector.

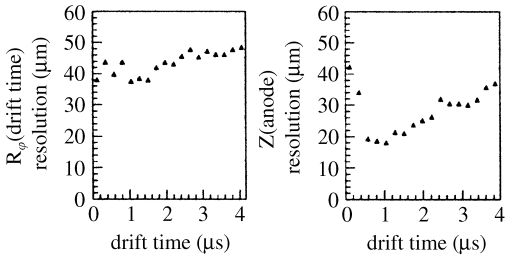

Fig. 15. Spatial resolution obtained with ALICE prototype Si drift chambers from time measurement and from anode pad segmentation.

good drift field homogeneity and precise on-sensor voltage dividers for drift cathodes. With drift chamber prototypes developed for the ALICE experiment spatial resolution between $\sigma = 40$ and 50 μm from time measurement and $\sigma = 20$–30 μm from anode segmentation have been demonstrated (Fig. 15). It can be seen that his device has a worse resolution for tracks close to the readout anodes.

5. Front-end electronics

The requirements on the amplifications of relatively weak signals from Si detectors are very different for the various types of sensors. The very high luminosities needed at LHC and TEVATRON put particularly difficult constraints on the performance of front-end electronics for Si pixel and strip detectors. Very low noise at high speed with a capability of storing all information recorded in the sensors until a level 1 trigger signal comes back to the front-end have to be achieved. Since the front-end electronics has to be in the same place as the sensors, strictly true for pixel devices, radiation hardness up to the highest fluences is needed. Availability of radiation hard technologies is of paramount importance.

Requirements on and architectures of front-end electronics for different experiments are mostly influenced by two main issues: first level trigger rate and occupancy. In collider experiments one can distinguish three scenarios:

(i) e^+e^- B-factories with trigger rates smaller than 1 kHz and low occupancy,
(ii) Hadron colliders with very high trigger rates in the order of 100 kHz–1 MHz and high occupancies.
(iii) A special case is heavy ion collider experiments with relatively low trigger rate but very high multiplicity.

In the first and third case relatively slow shaping times can, in principle, be used. Rather conventional low noise front-ends with multiplexed readout can be employed. In the second case, high bandwidth front-ends with long pipelines, and multiplexing are needed.

The thickness of Si sensors for tracking devices at LHC and TEVATRON can be between 200 μm for pixels and 300–400 μm for strip detectors. Multiple scattering and radiation damage, which leads to high voltages for full depletion, are the main limitations. The most probable signal for minimum ionising particles is therefore between 16,000 and 36,000 e–h pairs. This puts immediately a very strong requirement on the noise in front-ends.

5.1. Strip detectors

A practical length of a strip in LHC trackers has been chosen to be about 12 cm, which will result in a total load capacitance of 20–25 pF. Given the speed requirement, of about 25 ns shaping time, determined by occupancy, one needs to exploit the most suitable available technologies to achieve the lowest possible noise. Strong limitations in power dissipation put another constraint on front-end implementations. Typically one cannot exceed 5 mW/channel in order to be able to evacuate the heat in the densely packed geometries.

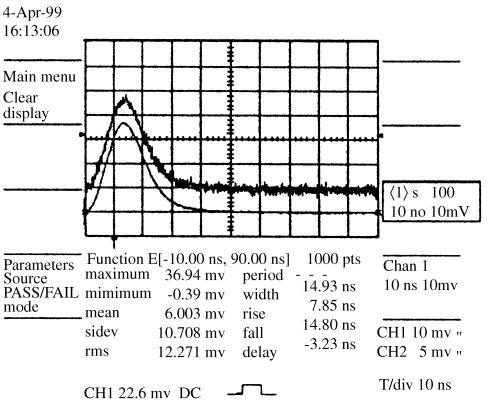

Fig. 16. Response to 4 fC input charge measured with a preamplifier designed in 0.25 μm technology. Peaking time $\tau_P = 13$ ns. Input capacitance about 5 pF [22].

Radiation hard technologies exist both for full CMOS and for BICMOS implementations. For load capacitance of the order of 20 pF and very short shaping times around 10 ns a bipolar input stage will exhibit lower series noise compared with an optimised CMOS input stage. This is essentially due to the fact that the transconductance of a bipolar junction transistor depends linearly on the collector current while in a CMOS FET it is proportional to SQRT $(2KT_dW/L)$. W and L are the width and length of the gate area and I_d is the drain current of the input FET. K is proportional to the gate oxide thickness [22,23].

In deep sub-micron CMOS processes one could expect a higher transconductance of the input FET in a charge sensitive preamplifier at the same drain current I_d and therefore an improved noise slope compared with 1 μm technologies. Moreover deep sub-micron FETs will operate close to the weak inversion regime, where the transconductance is directly proportional to I_d as it is the case for a bipolar junction transistor. First measurements on a test amplifier [22] give a result for the noise slope of 81 e^-/pF at 13 ns shaping time (Fig. 16). This is still about 50% higher than that measured with a bipolar amplifier in the SCTA chip [9], after scaling to the same shaping time.

The very short channel length $L = 0.35$ μm chosen in this design may contribute to the relatively high noise slope due to short channel effects [24].

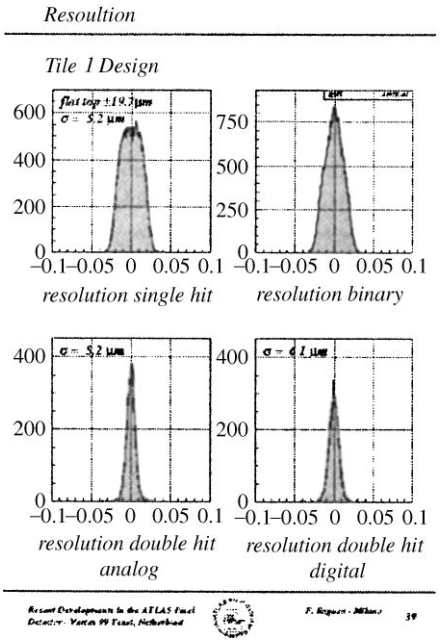

Fig. 17. Spatial resolution obtained with ATLAS pixel detector prototype, for co-ordinate in 50 μm pitch direction.

5.2. Pixel detectors

For pixel detectors in the LHC experiments the requirements are similar but the extremely high density and granularity of a pixel detector put even more stringent requirements on architectures and designs of the front-end. On a very small area, typically 15,000–20,000 μm^2, amplification and discrimination of small signals (thin substrates, signal loss after irradiation) has to be achieved at high speed with very-low power consumption, of the order of 50 μW/pixel. Noise occupancy cannot exceed about 10^{-6} hits per pixel per bunch crossing. Complicated peripheral logic is needed on a very small area to handle information from single columns at the periphery of a pixel chip. The electronics should survive more than 30 Mrad over 10 years. Fig. 17 gives an example of spatial resolution obtained with an ATLAS pixel readout chip.

6. Mechanics, cooling and alignment

The mechanical mounting, alignment and cooling of future LHC Si trackers will present many

Fig. 18. A drawing of the ATLAS pixel space frame.

new challenges. Double-sided Si strip detectors, which have an in-built front to back alignment determined by the processing in the foundry, are replaced by back-to-back mounted single-sided sensors. Precision mounting gigs will be used to guarantee back-to-front alignment of sensors on a module of a few microns. The necessary relative position accuracy of many modules mounted on ladder-type supports can be achieved with three dimensional (3-D) measuring machines with touch probes or optical sensors. One-micron precision can be obtained with industrial machines.

The overall mechanical support structure which holds, in the case of the very big LHC Si trackers, several thousand modules each made of several detectors, has to provide a position accuracy and stability much better than the point resolution. As an example, a drawing of the space frame, which will carry the pixel modules of the ATLAS Si tracker, is shown in Fig. 18.

New methods will have to be developed for measurement of fully assembled large trackers with area of more than $100\,m^2$. Thermal imaging and white light interferometric profile measurements are foreseen. Finally, software alignment with tracks will have to be used to determine relative positions of several thousand sensors with a precision of better than $10\,\mu m$.

In present day vertex detectors, cooling can be achieved with water cooling systems supplying the support end rings. In LHC trackers the challenge is much bigger since each module has to be cooled separately to temperatures below $0^\circ C$, so as to keep the leakage current and full depletion voltage after irradiation at a reasonably low value. It is believed that 2 phase evaporative systems are necessary to achieve stable and low temperatures.

7. Conclusion

From the first Si vertex detectors in fixed target experiments, which covered a few cm^2 areas, it took only 20 years to reach the construction phase of Si vertex detectors/trackers of more than $100\,m^2$. While the first small vertex detectors were exposed to very small radiation doses, the detectors planned for future will have to function in an extremely harsh radiation environment of total fluences up to several 10^{14} charged particles/cm^2. A whole decade of research was devoted to developing radiation hard sensors and front-end electronics, which can be operated at extreme speeds required by the high-luminosity interactions and can survive the radiation. At present, all the ingredients to build these challenging vertex detectors for future high-luminosity collider experiments are available. The biggest help to survive highest radiation levels probably came from outside high-energy physics in the form of the deep sub-micron CMOS technology. With relatively little specific developments by the HEP community, this technology can provide now the most radiation hard circuits for detector readout.

References

[1] E. Nygaard et al., Nucl. Instr. and Meth. A 301 (1991) 506.
[2] J. Straver et al., Nucl. Instr. and Meth. A 348 (1994) 485.
[3] C. Colledani et al., Nucl. Instr. and Meth. A 372 (1996) 379.
[4] N. Bingefors et al., Nucl. Instr. and Meth. A 328 (1993) 447.
[5] S. Tkaczyk, Nucl. Instr. and Meth. A 342 (1994) 240.
[6] G. Lutz, Semiconductor radiation detectors, Device Physics, Springer, Berlin, 1999 (Chapter 11), ISBN3-540-64859-3.
[7] R. Wunnstorf, Ph.D. Thesis, University of Hamburg, October 1992.
[8] M. Moll, Ph.D. Thesis, University of Hamburg, December 1999, DESY-THESIS-1999-040, ISN 1435-8085.
[9] E. Chesi et al., Performance of a 128 channel analogue front-end chip for read-out of Si strip detector modules for LHC experiments, Trans. Nucl. Sci., IEEE Conference, Seattle, 1999, to be published.
[10] Ch. Posch, Doctoral Thesis, Analog readout for the ATLAS semiconductor tracker, CERN, January 1999.
[11] Proceedings of Second Workshop on Electronics for LHC Experiments, Balatonfüred, Hungary, September 23–27, 1996 CERN/LHCC/96-39, p. 401–420.
[12] DMILL, A mixed analog-digital radiation-hard technology for high-energy physics electronics, RD29, Status Report, CERN/LHCC 97-15, March 1997.

[13] P. Jarron et al., Nucl. Phys. B (Proc. Suppl.) 78 (1999) 625.
[14] N.S. Saks, M.G. Ancona, J.A. Modalo, IEEE Trans. Nucl. Sci. NS-31 (1984) 1249.
[15] The GaAs Collaboration, CERN/LHCC 97-37, Status Report RD8, 10 July 1997.
[16] The ROSE Collaboration, CERN/LHCC 2000-009, LEB Status Report/RD48, 31 December 1999.
[17] W. Adam et al., Micro-strip Sensors Based on CVD Diamond, Preprint, CERN-EP-2000-041, March 9, 2000.
[18] R. Bailey, C.J.S. Damerell et al., Nucl. Instr. and Meth. 213 (1983) 201.
[19] K. Abe et al., Nucl. Instr. and Meth. A 400 (1997) 287.
[20] P. Weilhammer, Nucl. Instr. and Meth. A 383 (1996) 89.
[21] P. Rehak et al., Nucl. Instr. and Meth. A 235 (1985) 224.
[22] A. Rivetti et al., Proceedings of the Fifth Workshop on Electronics for LHC Experiments, CERN 99-09, CERN/LHCC/99-33, October 1999, pp. 157–161.
[23] P. Weilhammer, Nucl. Instr. and Meth. A 433 (1999) 413.
[24] Z.Y. Yang, W.M.C. Sansen, Low Noise Wide-Band Amplifier in Bipolar and CMOS Technologies, Kluwer Academic Publishers, Dordrecht, 1991.